Receptor for Advanced Glycation End Products (RAGE) Deficiency Attenuates the Development of Atherosclerosis in Diabetes

Aino Soro-Paavonen,[1] Anna M.D. Watson,[1] Jiaze Li,[1] Karri Paavonen,[1] Audrey Koitka,[1] Anna C. Calkin,[1] David Barit,[1] Melinda T. Coughlan,[1] Brian G. Drew,[2] Graeme I. Lancaster,[3] Merlin Thomas,[1] Josephine M. Forbes,[1] Peter P. Nawroth,[4] Angelika Bierhaus,[4] Mark E. Cooper,[1] and Karin A. Jandeleit-Dahm[1]

OBJECTIVE—Activation of the receptor for advanced glycation end products (RAGE) in diabetic vasculature is considered to be a key mediator of atherogenesis. This study examines the effects of deletion of *RAGE* on the development of atherosclerosis in the diabetic apoE$^{-/-}$ model of accelerated atherosclerosis.

RESEARCH DESIGN AND METHODS—ApoE$^{-/-}$ and RAGE$^{-/-}$/apoE$^{-/-}$ double knockout mice were rendered diabetic with streptozotocin and followed for 20 weeks, at which time plaque accumulation was assessed by en face analysis.

RESULTS—Although diabetic apoE$^{-/-}$ mice showed increased plaque accumulation (14.9 ± 1.7%), diabetic RAGE$^{-/-}$/apoE$^{-/-}$ mice had significantly reduced atherosclerotic plaque area (4.9 ± 0.4%) to levels not significantly different from control apoE$^{-/-}$ mice (4.3 ± 0.4%). These beneficial effects on the vasculature were associated with attenuation of leukocyte recruitment; decreased expression of proinflammatory mediators, including the nuclear factor-κB subunit *p65*, *VCAM-1*, and *MCP-1*; and reduced oxidative stress, as reflected by staining for nitrotyrosine and reduced expression of various NADPH oxidase subunits, *gp91phox*, *p47phox*, and *rac-1*. Both RAGE and RAGE ligands, including S100A8/A9, high mobility group box 1 (HMGB1), and the advanced glycation end product (AGE) carboxymethyllysine were increased in plaques from diabetic apoE$^{-/-}$ mice. Furthermore, the accumulation of AGEs and other ligands to RAGE was reduced in diabetic RAGE$^{-/-}$/apoE$^{-/-}$ mice.

CONCLUSIONS—This study provides evidence for RAGE playing a central role in the development of accelerated atherosclerosis associated with diabetes. These findings emphasize the potential utility of strategies targeting RAGE activation in the prevention and treatment of diabetic macrovascular complications. ***Diabetes*** **57:2461–2469, 2008**

From the [1]Albert Einstein Juvenile Diabetes Research Foundation Centre for Diabetes Complications, Diabetes Metabolism Division, Baker Heart Research Institute, Melbourne, Australia; the [2]Clinical Physiology Laboratory, Baker Heart Research Institute, Melbourne, Australia; the [3]Cellular and Molecular Metabolism Laboratory, Baker Heart Research Institute, Melbourne, Australia; and the [4]Department of Medicine I and Clinical Chemistry, University of Heidelberg, Heidelberg, Germany.

Corresponding author: Karin Jandeleit-Dahm, karin.jandeleit-dahm@baker.edu.au.

Received 21 December 2007 and accepted 20 May 2008.

Published ahead of print at http://diabetes.diabetesjournals.org on 28 May 2008. DOI: 10.2337/db07-1808.

The receptor for advanced glycation end products (RAGE) is a multiligand cell surface molecule belonging to the immunoglobulin superfamily (1). It is expressed as full-length, N-truncated, and C-truncated isoforms, generated in humans by alternative splicing (2). Activation of the full-length RAGE receptor has been implicated in a range of chronic diseases, including various diabetic complications and atherosclerosis (1). In particular, studies in RAGE$^{-/-}$ mice that carry the dominant-negative form of the receptor (2–6) and in RAGE-overexpressing mice (7) have confirmed an important role of RAGE activation in the development of diabetic nephropathy, neuropathy, and impaired angiogenesis. RAGE activation has also been implicated in the acceleration of atherosclerotic lesion formation as well as in the maintenance of proinflammatory and prothrombotic mechanisms, characteristic of diabetes-accelerated atherosclerosis (8,9). RAGE also represents an important mediator of oxidative stress in diabetes. Activation of RAGE in vitro leads to increased NADPH oxidase expression, mitochondrial oxidase activity, and downregulation of endogenous antioxidant activity (10,11). RAGE$^{-/-}$ mice have a suppression of neointimal proliferation after externally induced arterial injury in the absence of diabetes (12). Moreover, blockade of RAGE-dependent signaling by soluble RAGE (sRAGE) has been shown to inhibit the progression of atherosclerotic changes (8,9) and kidney disease (3) in diabetic mice, possibly by suppressing the activation of nuclear factor-κB (NF-κB) activation and inflammatory cytokine expression. The present study examined the role of RAGE in the development of diabetes-accelerated atherosclerosis in a model of insulin deficiency, the streptozotocin-induced diabetic RAGE$^{-/-}$/apoE$^{-/-}$ mouse. Our aim was to determine the effect of global RAGE deficiency, which includes absence of both the full-length receptor and endogenous sRAGE on the development of vascular lesions in the presence and absence of diabetes. Furthermore, key mediators of the atherosclerotic process in diabetes were examined, and the effects on these pathways were assessed in these RAGE-deficient mice.

RESEARCH DESIGN AND METHODS

This study used the well-characterized apoE$^{-/-}$ mouse model of accelerated atherosclerosis, whereby mice develop complex vascular lesions after 20 weeks of diabetes that resemble the morphology seen in human atherosclerosis (9,13–15). Six-week-old male apoE$^{-/-}$ mice (backcrossed 20 times to a C57BL/6 background; Animal Resource Centre, Canning Vale, Western Aus-

TABLE 1
Metabolic parameters of the groups at week 20

Parameters	Control apoE$^{-/-}$	Diabetic apoE$^{-/-}$	Control RAGE$^{-/-}$/apoE$^{-/-}$	Diabetic RAGE$^{-/-}$/apoE$^{-/-}$
n	10	10	10	10
GHb (%)*	3.8 ± 0.1	15.8 ± 0.7†	4.5 ± 0.2†‡	15.0 ± 0.4§
Body weight (g)*	30.7 ± 0.4	24.5 ± 0.6†	38.4 ± 1.1†‡	27.7 ± 0.5‡§
Plasma glucose (mmol/l)	11.3 ± 0.9	31.2 ± 1.2†	9.6 ± 1.2‡	31.0 ± 1.9§
Total cholesterol (mmol/l)	14.0 ± 1.1	25.6 ± 2.1†	12.7 ± 0.6‡	21.1 ± 1.2§
HDL cholesterol (mmol/l)	2.6 ± 0.2	3.1 ± 0.4	3.1 ± 0.2	4.0 ± 0.3§
LDL cholesterol (mmol/l)	10.0 ± 1.0	21.6 ± 1.9†	8.8 ± 0.4‡	16.5 ± 0.8‡§
Triglycerides (mmol/l)	1.8 ± 0.3	2.1 ± 0.3	1.9 ± 0.4	1.4 ± 0.2

Data are means ± SE. *GHb and weight measurements performed in 24 animals/group. †$P < 0.001$ vs. control apoE$^{-/-}$ group; ‡$P < 0.05$ vs. diabetic apoE$^{-/-}$ group; §$P < 0.05$ vs. control RAGE$^{-/-}$/apoE$^{-/-}$.

tralia) and RAGE$^{-/-}$/apoE$^{-/-}$ mice, generated by backcrossing RAGE$^{-/-}$ mice (16) on the C57BL/6 background into apoE$^{-/-}$ mice on the same background for 10 generations (University of Heidelberg, Heidelberg, Germany) (Supplementary Fig. 1, available in an online appendix at http://dx.doi.org/10.2337/db07-1808), were housed at the Precinct Animal Centre at Baker Heart Research Institute and studied according to National Health and Medical Research Council (NHMRC) guidelines. Mice (n = 24/group) were rendered diabetic via five daily intraperitoneal injections of 55 mg/kg streptozotocin (Boehringer, Mannheim, Germany) per day, resulting in insulin deficiency (13). Control animals received vehicle (citrate buffer) alone. All animals were followed for 20 weeks. Mice were allowed access to standard mouse chow and water ad libitum. Mice were killed using an intraperitoneal injection of 100 mg/kg Euthal (Delvet, Seven Hills, Australia), followed by exsanguination by cardiac puncture. Excised aortas (n = 10–14) were placed in 10% neutral buffered formalin and quantitated for lesion area before being embedded in paraffin for immunohistochemical analysis. In the remaining mice (n = 10–14), aortas were snap-frozen in liquid nitrogen and stored at −70°C for subsequent RNA extraction. At the conclusion of the study, GHb was measured by high-performance liquid chromatography (17). Total plasma cholesterol, HDL, and triglyceride concentrations were measured in 9–10 mice per group by autoanalyzer. LDL cholesterol was calculated by the Friedewald formula. The S100 A8/A9 ELISA kit (Immundiagnostik, Bensheim, Germany) was used to measure this S100 isoform in plasma according to the manufacturer's instructions. A Quantitative ELISA (Shino-Test, Tokyo) was used to measure plasma high mobility group box 1 (HMGB1) concentration.

Plaque area quantitation. Plaque area was quantitated as described previously (13,15). In brief, aortas (n = 10–14 aortas/group) were cleaned of excess fat under a dissecting microscope and subsequently stained with Sudan IV-Herxheimer's solution (0.5% wt/vol) (Gurr; BDH, Poole, U.K.). Aortas were dissected longitudinally; divided into arch, thoracic, and abdominal segments; and pinned flat onto wax. Images were acquired with a dissecting microscope equipped with an Axiocam camera (Zeiss, Heidelberg, Germany). Total and segmental plaque area was quantitated as a percentage area of aorta stained (Adobe Photoshop version 7.0). Tissue was subsequently embedded in paraffin, and sections were cut for immunohistochemical analysis.

Real-time RT-PCR. Total RNA was extracted from whole aorta by homogenizing (Polytron PT-MR2100; Kinematica, Littau-Lucerne, Switzerland) in TRIzol (Life Technologies, Rockville, MD). Total RNA was then DNase-treated (DNA removal kit; Ambion, Austin, TX), and cDNA was synthesized by reverse transcription (Pierce Biotechnology, Rockford, IL). Quantitative real-time RT-PCR was performed using the Taqman System on an ABI Prism 7500 Sequence Detector (Applied Biosystems, Foster City, CA) and analyzed using software detection systems (SDS version 1.9) software. Gene expression was normalized to 18S rRNA (Applied Biosystems). Detailed information on probes is provided in Supplementary Table 1. For each analysis, 10–14 animals per group were used.

Immunohistochemistry. Serial 4-μm sections were stained for α-smooth muscle actin (α-SMA) (1:200; DakoCytomation, Carpinteria, CA), the macrophage marker F4/80 (1:50; Serotec, Oxford, U.K.), nitrotyrosine (1:50; Chemicon, Temecula, CA), S100A8/A9 (1:250; Immundiagnostik), HMGB1 (1:1,000; Abcam, Cambridge, U.K.), carboxymethyllysine (CML) (1:1,000; Abcam), the T-cell marker CD3 (1:50; Abcam), collagens III and IV (goat anti-human collagen III and IV; 1:75 and 1:800, respectively; SouthernBiotech, Birmingham, AL), vascular cell adhesion molecule-1 (VCAM-1) (1:50; Pharmingen, San Diego, CA), and monocyte chemotactic protein-1 (MCP-1) (1:500; R&D Systems, Minneapolis, MN). Enzymatic trypsin antigen retrieval was used for F4/80, pepsin digestion in 0.01 mol/l HCl was used for collagen III and IV, and heat-induced antigen retrieval in 0.01 mol/l citric acid (pH 6.0) was applied for HMGB1 and CD3 antibodies. Sections were incubated with the primary antibody overnight at 4°C. Secondary antibody, biotinylated anti-mouse IgG (Vector Laboratories, Burlingame, CA), anti-rat immunoglobulin (Vector Laboratories), anti-rabbit IgG (Vector Laboratories), or anti-goat IgG (Vector Laboratories) were added 1:200 to 1:500 to sections for 30 min at room temperature. This was followed by Vectastain ABC Elite reagent (Vector Laboratories) or alternatively catalyzed signal amplification (DakoCytomation). Peroxidase activity was identified by reaction with 3,3′-diaminobenzidine tetrahydrochloride (Sigma-Aldrich, St. Louis, MO) or 3-amino-9-ethylcarbazole (Vector Laboratories) substrate. Sections were counterstained with Mayer's hematoxylin when appropriate. Staining was quantitated from digital microscope photographs as percent of positively stained tissue using ImagePro 6.0 software. For each analysis, 7–10 animals per group were used.

Western blotting. Total lysates from mouse aorta were subjected to 10–12% SDS-PAGE and transferred onto polyvinylidene difluoride membranes. The membranes were incubated with mouse monoclonal anti–MCP-1 antibody (R&D Systems) at 1 μg/ml or mouse monoclonal anti–β-actin (Abcam) at 1/10,000 dilution. The membranes were washed with Tris-buffered saline with Tween and then incubated with EnVision+ System–HRP-Labeled Polymer anti-mouse secondary antibody at 1/25 (DakoCytomation). Immunoreactivity was detected using an enhanced chemiluminescence kit (Sigma-Aldrich).

Statistical analysis. Data were analyzed by ANOVA using SPSS 15.0 software. Post hoc comparisons were made among the various groups using Fishers least significant difference method. Data are expressed as means ± SE unless otherwise specified. $P < 0.05$ was considered to be statistically significant.

RESULTS

Metabolic parameters. The induction of diabetes in both RAGE$^{-/-}$/apoE$^{-/-}$ and apoE$^{-/-}$ mice resulted in increased plasma glucose and GHb concentrations, which were comparable between the diabetic groups (Table 1). Plasma concentrations of total and LDL cholesterol levels were also significantly increased in both groups following the induction of diabetes, although this increase was attenuated in RAGE$^{-/-}$/apoE$^{-/-}$ mice.

Plaque accumulation. The induction of diabetes in apoE$^{-/-}$ mice led to a significant (approximately fourfold) increase in total atherosclerotic plaque area. However, this diabetes-associated increase in plaque area was completely prevented in diabetic RAGE$^{-/-}$/apoE$^{-/-}$ mice, with plaque accumulation not significantly different from that seen in control apoE$^{-/-}$ mice (Fig. 1*A*). The reduction in the plaque accumulation in diabetic RAGE$^{-/-}$/apoE$^{-/-}$ mice was observed at all three aortic sites: the arch, thoracic, and abdominal aortas. In addition, there was a further reduction in plaque area in nondiabetic RAGE$^{-/-}$/apoE$^{-/-}$ mice when compared with control apoE$^{-/-}$ mice (Fig. 1*A* and *B*).

Plaque morphology and smooth muscle cell recruitment. The induction of diabetes was not only associated with plaque accumulation, but, in addition, diabetic plaque was also significantly more complex, characterized by

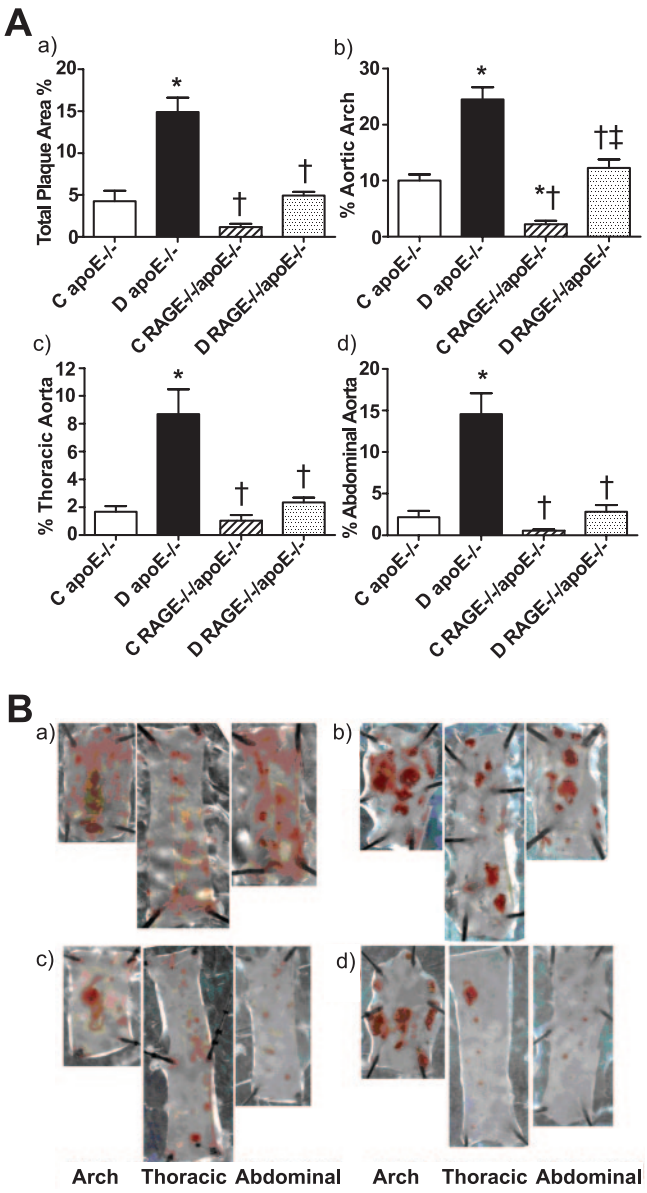

FIG. 1. *A*: **Quantitation of atherosclerotic plaque area (%) of aortic segments by the en face method in total aorta (*a*), aortic arch (*b*), thoracic aorta (*c*), and abdominal aorta (*d*). *$P < 0.01$ vs. control apoE$^{-/-}$, †$P < 0.01$ vs. diabetic apoE$^{-/-}$, ‡$P < 0.05$ vs. control RAGE$^{-/-}$/apoE$^{-/-}$. *B*: Representative photomicrographs of aortas from control apoE$^{-/-}$ (*a*), diabetic apoE$^{-/-}$ (*b*), control RAGE$^{-/-}$/apoE$^{-/-}$ (*c*), and diabetic RAGE$^{-/-}$/apoE$^{-/-}$ (*d*) using the en face technique. Lesions are shown in red after Sudan IV staining. (Please see http://dx.doi.org/10.2337/db07-1808 for a high-quality digital representation of this figure.)**

increased accumulation of foam cells, cholesterol clefts, and leukocyte recruitment similar to that seen in human disease. Furthermore, atherosclerotic plaque in diabetic apoE$^{-/-}$ mice involves the proliferation and migration of medial vascular smooth muscle cells into the vessel intima, as demonstrated by increased expression of α-SMA protein when compared with control apoE$^{-/-}$ mice (Supplementary Fig. 2). However, the atherosclerotic plaque in diabetic RAGE$^{-/-}$/apoE$^{-/-}$ mice was significantly less complex, with reduced α-SMA expression when compared with diabetic apoE$^{-/-}$ mice.

Vascular accumulation of macrophages and T-cells. Leukocyte recruitment is a key component of vascular inflammation and atherogenesis. In our study, there was increased CD3 staining in the vessel wall of the diabetic apoE$^{-/-}$ mice, consistent with accumulation of T-cells (Fig. 2*A* and *B*). T-cell recruitment associated with diabetes was significantly decreased in the RAGE$^{-/-}$/apoE$^{-/-}$ mice to levels not significantly different from control apoE$^{-/-}$ mice, with control RAGE$^{-/-}$/apoE$^{-/-}$ mice showing an additional reduction in vascular T-cell recruitment. Similarly, macrophage accumulation, as detected by staining with the F4/80 marker, was significantly increased in diabetic apoE$^{-/-}$ mice compared with controls (Fig. 2*C* and *D*). Macrophage accumulation was also reduced in the diabetic RAGE$^{-/-}$/apoE$^{-/-}$ mice when compared with diabetic apoE$^{-/-}$ mice. Macrophage staining was detected in both the vascular wall and the fibrous cap of the atherosclerotic lesions, particularly in diabetic apoE$^{-/-}$ mice.

Markers of vascular inflammation. To explore the potential mechanisms responsible for vascular protection in our model, we studied the aortic gene transcription of various proteins that have previously been linked to generation of vascular lesions (9,18,19). In particular, vascular inflammation is thought to be the key initiator of atherosclerosis in both experimental and human disease. Accelerated atherosclerosis in diabetic apoE$^{-/-}$ mice was associated with increased aortic expression of the proinflammatory transcription factor NF-κB subunit *p65*, *MCP-1*, *VCAM-1*, *tissue factor*, and the renin-angiotensin system (RAS)-related C3 botulinum substrate 1 (*rac1*) (Table 2). Reduction in plaque area in RAGE$^{-/-}$/apoE$^{-/-}$ mice was also associated with a significant reduction in gene expression of these proatherosclerotic mediators to levels similar to those observed in control apoE$^{-/-}$ aortas (Table 2). By immunohistochemistry, MCP-1 expression was increased at least twofold in diabetic apoE$^{-/-}$ mice particularly within the plaque, specifically foam cells and macrophages, and this increase was not seen in the aortas from diabetic RAGE$^{-/-}$/apoE$^{-/-}$ mice (Supplementary Fig. 3*A* and *B*). In addition, Western blot analysis showed that MCP-1 protein expression was increased twofold in aortic extracts from diabetic apoE$^{-/-}$ mice, and this increased expression was significantly reduced in the aortas from diabetic RAGE$^{-/-}$/apoE$^{-/-}$ (Supplementary Fig. 3*C*). Aortic VCAM-1 protein expression was also assessed by immunohistochemistry. Diabetic apoE$^{-/-}$ mice had significantly increased vascular VCAM-1 staining, including within endothelial cells, and this was not seen in control apoE$^{-/-}$ mice or diabetic and control RAGE$^{-/-}$/apoE$^{-/-}$ mice (Supplementary Fig. 4).

Expression of collagens and matrix metalloproteinases. Gene expression of *collagen I*, *III*, *IV* (*α I*), and *IVα III* were increased in the diabetic apoE$^{-/-}$ aorta compared with the control apoE$^{-/-}$ aorta (Table 2). Collagen III gene expression was significantly decreased in the diabetic RAGE$^{-/-}$/apoE$^{-/-}$ aorta when compared with diabetic apoE$^{-/-}$ mice. We also assessed collagen protein expression in the vascular wall by immunohistochemistry, specifically assessing the fibrillar type III collagen and the basement membrane type IV collagen. Diabetic apoE$^{-/-}$ mice have significantly increased vascular collagen III and collagen IV deposition compared with control apoE$^{-/-}$ mice (Supplementary Figs. 5 and 6). The diabetic RAGE$^{-/-}$/apoE$^{-/-}$ mice had significantly less collagen III and IV staining.

We also examined the gene expression of matrix metalloproteinases 2 and 9 (*MMP-2* and *MMP-9*, respectively) that are involved in the inflammatory response and in

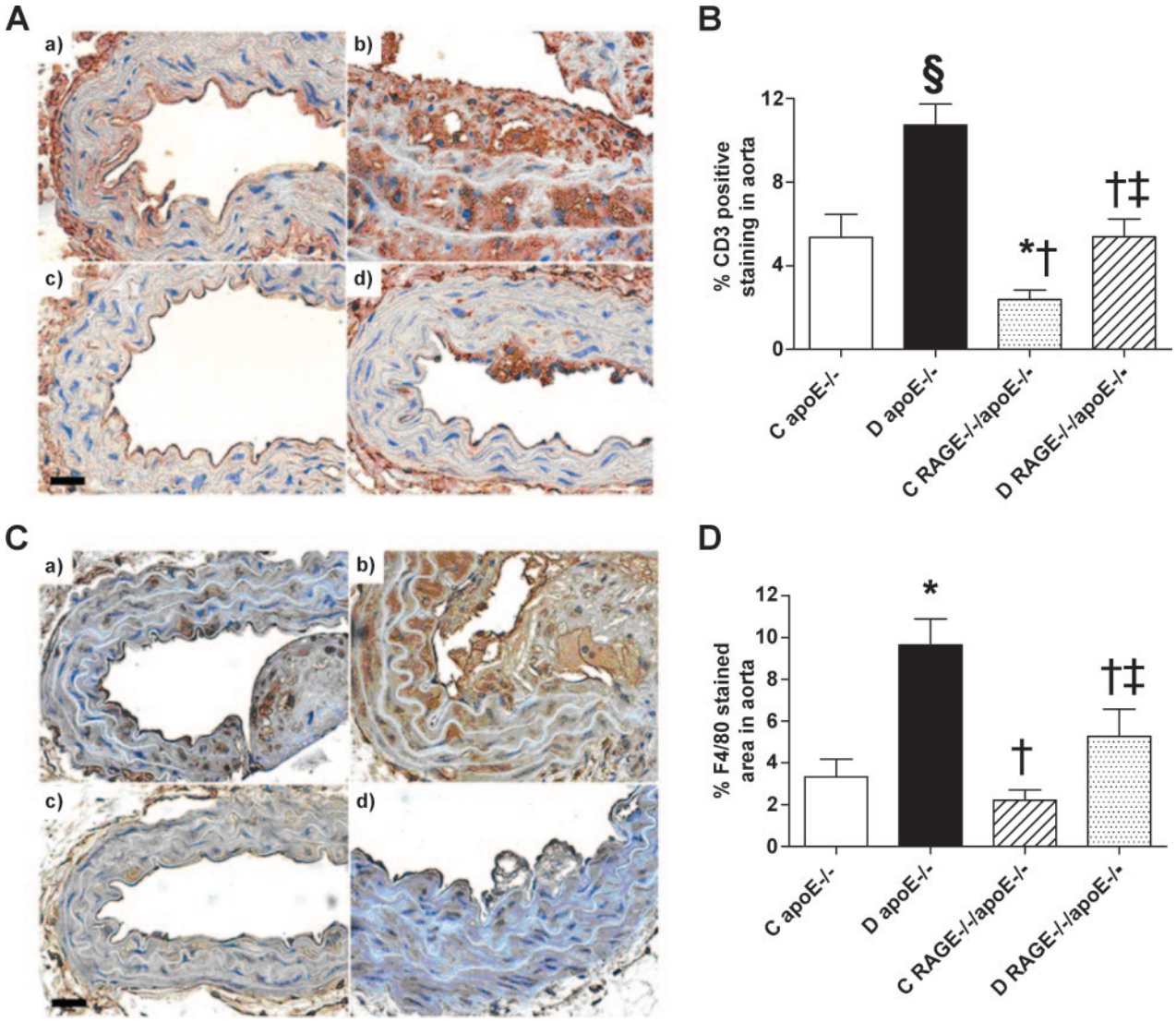

FIG. 2. ***A*: Representative aortic sections showing anti-CD3 staining demonstrating T-cell accumulation in control apoE$^{-/-}$ (*a*), diabetic apoE$^{-/-}$ (*b*), control RAGE$^{-/-}$/apoE$^{-/-}$ (*c*), and diabetic RAGE$^{-/-}$/apoE$^{-/-}$ (*d*) mice. Scale bar = 20 μm. *B*: Graph presenting percentage of CD3-positive staining in each group. **P* < 0.05 vs. control apoE$^{-/-}$, †*P* < 0.001 vs. diabetic apoE$^{-/-}$, ‡*P* < 0.05 vs. control RAGE$^{-/-}$/apoE$^{-/-}$. §*P* < 0.001 vs. control apoE$^{-/-}$. Data are means ± SE. *C*: Representative aortic sections of F4/80 staining demonstrating macrophage infiltration in control apoE$^{-/-}$ (*a*), diabetic apoE$^{-/-}$ (*b*), control RAGE$^{-/-}$/apoE$^{-/-}$ mice (*c*), and diabetic RAGE$^{-/-}$/apoE$^{-/-}$ (*d*). Scale bar = 20 μm. *D*: Graph presenting percentage of F4/80-positive staining in each group. **P* < 0.001 vs. control apoE$^{-/-}$, †*P* < 0.01 vs. diabetic apoE$^{-/-}$, ‡*P* < 0.05 vs. control RAGE$^{-/-}$/apoE$^{-/-}$. Data are means ± SE. (Please see http://dx.doi.org/10.2337/db07-1808 for a high-quality digital representation of this figure.)**

collagen degradation (20). There was a threefold induction in the expression of *MMP-2* and a twofold induction in the expression of *MMP-9* in the diabetic apoE$^{-/-}$ aorta compared with the control apoE$^{-/-}$ aorta. *MMP-9* gene expression was significantly attenuated in diabetic RAGE$^{-/-}$/apoE$^{-/-}$ aorta, whereas *MMP-2* gene expression was similar to that seen in diabetic apoE$^{-/-}$ aorta.

Accumulation of RAGE ligands. The accumulation of a range of RAGE ligands, including the advanced glycation end product (AGE), CML, HMGB1, and S100A8/A9, in settings such as diabetes are considered to play a role in progressive vascular injury. As expected, diabetic apoE$^{-/-}$ mice had a significant elevation in vascular AGE deposition when compared with the nondiabetic apoE$^{-/-}$ animals, as detected by immunostaining for the well-described AGE, CML (Fig. 3). CML immunostaining was reduced in the aortas of diabetic RAGE$^{-/-}$/apoE$^{-/-}$ mice to levels not significantly different from control animals. A similar pattern was seen with respect to another RAGE ligand, HMGB1 (1), with increased expression in diabetic apoE$^{-/-}$ aorta when compared with the control apoE$^{-/-}$ mice, with normalization in RAGE$^{-/-}$/apoE$^{-/-}$ mice (Fig. 4). We also measured plasma HMGB1 concentrations. Interestingly, plasma HMGB1 levels were higher in diabetic RAGE$^{-/-}$/apoE$^{-/-}$ mice compared with diabetic apoE$^{-/-}$ mice (369 ± 44 vs. 201 ± 13 ng/ml, $P < 0.05$). Nondiabetic RAGE$^{-/-}$/apoE$^{-/-}$ mice tended to have slightly higher circulating HMGB1 levels than nondiabetic apoE$^{-/-}$ mice (356 ± 63 vs. 235 ± 28 ng/ml, $P = 0.11$).

The diabetic apoE$^{-/-}$ mice had significantly increased positive staining of the proinflammatory cytokine, S100A8/A9, a known RAGE ligand (21) when compared with control animals (Fig. 5*A* and *B*), with prominent staining appearing in the aortic lesions, particularly within macrophages, foam cells, and endothelial cells. In the RAGE$^{-/-}$/apoE$^{-/-}$ mice, the aortic expression of S100A8/A9 protein was significantly decreased when compared with diabetic apoE$^{-/-}$ aortas. The diabetic apoE$^{-/-}$ mice also had a significant elevation in circulating levels of S100A8/A9 when compared with control animals (Fig. 5*C*). In the

TABLE 2
Gene expression of proatherogenic mediators in the aorta

Parameters	Control apoE$^{-/-}$	Diabetic apoE$^{-/-}$	Control RAGE$^{-/-}$/apoE$^{-/-}$	Diabetic RAGE$^{-/-}$/apoE$^{-/-}$
n	12	10	14	14
Inflammatory mediators				
p65	1.0 ± 0.1	2.6 ± 0.5*	1.0 ± 0.1†	1.5 ± 0.2*†
VCAM-1	1.0 ± 0.2	4.2 ± 0.6*	1.7 ± 0.2*†	1.6 ± 0.4†
MCP-1	1.0 ± 0.2	6.2 ± 1.3*	1.7 ± 0.4*†	2.6 ± 0.7*†
Tissue factor	1.0 ± 0.2	2.9 ± 0.7*	0.6 ± 0.3†	1.7 ± 0.4‡
NADPH oxidase and RAS				
p47phox	1.0 ± 0.2	5.1 ± 0.7*	1.0 ± 0.2†	1.8 ± 0.3*†‡
gp91phox	1.0 ± 0.3	3.54 ± 0.5*	1.22 ± 0.3†	2.1 ± 0.3*†‡
rac1	1.0 ± 0.1	1.5 ± 0.2*	1.4 ± 0.1	1.3 ± 0.2†
AT1a	1.0 ± 0.2	5.3 ± 1.3*	1.2 ± 0.3†	1.4 ± 0.3†
AGE receptors				
RAGE	1.0 ± 0.1	4.4 ± 1.1*	0	0
AGE-R1	1.0 ± 0.1	2.4 ± 0.3*	1.1 ± 0.1†	1.4 ± 0.2†
AGE-R2	1.0 ± 0.1	2.1 ± 0.4*	1.2 ± 0.1	1.7 ± 0.2
AGE-R3	1.0 ± 0.3	4.6 ± 1.1*	0.9 ± 0.1	1.8 ± 0.3†
CD36	1.0 ± 0.5	2.1 ± 0.4*	0.8 ± 0.1†	1.0 ± 0.2†
Indicators of matrix accumulation and degradation				
Collagen I	1.0 ± 0.1	4.1 ± 1.1*	1.2 ± 0.1†	3.1 ± 0.6*‡
Collagen III	1.0 ± 0.2	8.9 ± 2.9*	1.7 ± 0.2*†	2.8 ± 0.6*†
Collagen IV (αI)	1.0 ± 0.1	2.9 ± 0.7*	1.6 ± 0.2*†	2.7 ± 0.6*
Collagen IV (αIII)	1.0 ± 0.1	3.7 ± 1.2*	3.0 ± 0.7*	2.3 ± 0.4*
MMP-2	1.0 ± 0.2	3.0 ± 0.6*	1.2 ± 0.3†	2.1 ± 0.6
MMP-9	1.0 ± 0.2	1.9 ± 0.4*	1.1 ± 0.3	0.8 ± 0.2†

Data are means ± SE. *$P < 0.05$ vs. control apoE$^{-/-}$ group; †$P < 0.05$ vs. diabetic apoE$^{-/-}$ group; ‡$P < 0.05$ vs. control RAGE$^{-/-}$/apoE$^{-/-}$.

RAGE$^{-/-}$/apoE$^{-/-}$ mice, S100A8/A9 levels were similar to those seen in control mice.

Expression of AGE receptors. As previously described (14,15), the expression of full-length RAGE in apoE$^{-/-}$ mice was significantly increased after the induction of diabetes (Table 2), with focal expression overlying atherosclerotic plaque (data not shown). There was no *RAGE* expression in RAGE$^{-/-}$/apoE$^{-/-}$ aorta. The induction of diabetes was also associated with increased expression of AGE clearance receptors, including *AGE-R1* (oligosaccharyl transferase-48), *AGE-R3* (galectin-3), and the type B macrophage scavenger receptor, *CD36*. However, in RAGE$^{-/-}$/apoE$^{-/-}$ mice, the increased gene expression of these other AGE receptors was significantly attenuated (Table 2).

NADPH oxidase and oxidative stress in the vascular wall. We determined the potential impact of RAGE on the superoxide-generating NADPH oxidase in the diabetic vasculature. Interestingly, diabetes induced a 5.3-fold increase in expression of NADPH oxidase subunit *p47phox* and a 3.5-fold increase in *gp91phox* expression in the apoE$^{-/-}$ aorta, whereas in diabetic RAGE$^{-/-}$/apoE$^{-/-}$ double knockout mice, this upregulation of NADPH oxidase subunits was attenuated (Table 2). Diabetic apoE$^{-/-}$ mice also had increased expression of nitrotyrosine in their aortas, suggesting increased peroxynitrite-mediated protein oxidation (Fig. 6). Diabetes did not lead to a similar increase in nitrotyrosine staining in the RAGE$^{-/-}$/apoE$^{-/-}$ mice.

AT1 receptor expression. Reflecting an activated vascular RAS, which is known to upregulate NADPH-oxidase–dependent reactive oxygen species (ROS) generation (22), diabetic apoE$^{-/-}$ mice had a marked increase in gene expression of the angiotensin II type 1a receptor (*AT1a*). Aortic *AT1a* gene expression was significantly reduced in diabetic RAGE$^{-/-}$/apoE$^{-/-}$ mice when compared with diabetic apoE$^{-/-}$ mice (Table 2).

DISCUSSION

Atherosclerotic vascular disease is a major cause of morbidity and mortality in the diabetic population with accelerated plaque accumulation and vascular inflammation. Although a number of mechanisms have been postulated to contribute to the development and progression of atherosclerotic disease in diabetes, in the present study, we provide evidence that RAGE-dependent pathways play a central role in promoting vascular lesions in a rodent model of advanced atherosclerosis, the diabetic apoE$^{-/-}$ mouse. Our results show for the first time that the absence of *RAGE* suppresses diabetes-accelerated atherosclerosis. Our group has previously shown that the atherosclerotic plaques seen in diabetic apoE$^{-/-}$ mice resemble the complex morphology seen in patients with diabetes, including enhanced accumulation of macrophages, foam cells, and cholesterol clefts within the fatty atheroma and increased expression of inflammatory markers, proinflammatory cytokines, and chemokines (14,15,18). Without normalizing glucose or lipid levels, we show that in the absence of both full-length and sRAGE expression in diabetic RAGE$^{-/-}$/apoE$^{-/-}$ double knockout mice, the extent of plaque accumulation, vascular inflammation, and oxidative stress was significantly reduced to levels similar to those observed in control apoE$^{-/-}$ mice. In addition, atherosclerosis was further reduced in control RAGE$^{-/-}$/apoE$^{-/-}$ mice. These data are consistent with previous studies in nondiabetic RAGE$^{-/-}$ mice. RAGE$^{-/-}$ mice demonstrated suppression of neointimal expansion after

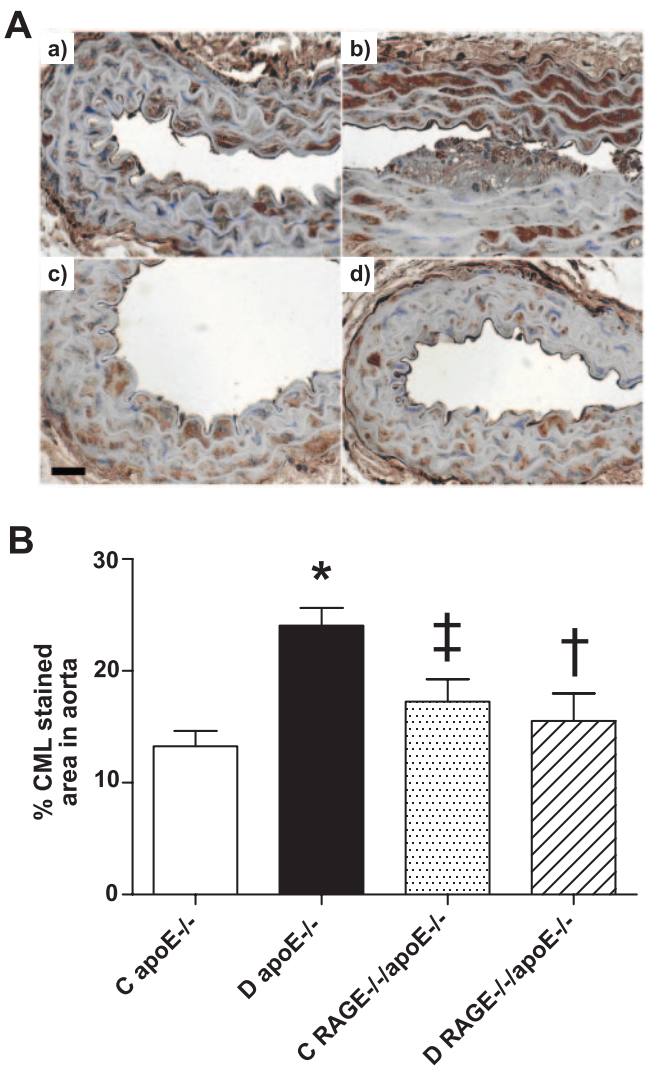

FIG. 3. *A*: Representative aortic sections demonstrating increased CML staining in the diabetic apoE$^{-/-}$ aorta. Panel presents aorta from control apoE$^{-/-}$ (*a*), diabetic apoE$^{-/-}$ (*b*), control RAGE$^{-/-}$/apoE$^{-/-}$ (*c*), and diabetic RAGE$^{-/-}$/apoE$^{-/-}$ (*d*) mice. Scale bar = 20 μm. *B*: Graph presenting percentage of CML-positive aortic area in each group. *P < 0.001 vs. control apoE$^{-/-}$, †P < 0.01 vs. diabetic apoE$^{-/-}$, ‡P < 0.05 vs. diabetic apoE$^{-/-}$. Data are means ± SE. (Please see http://dx.doi.org/10.2337/db07-1808 for a high-quality digital representation of this figure.)

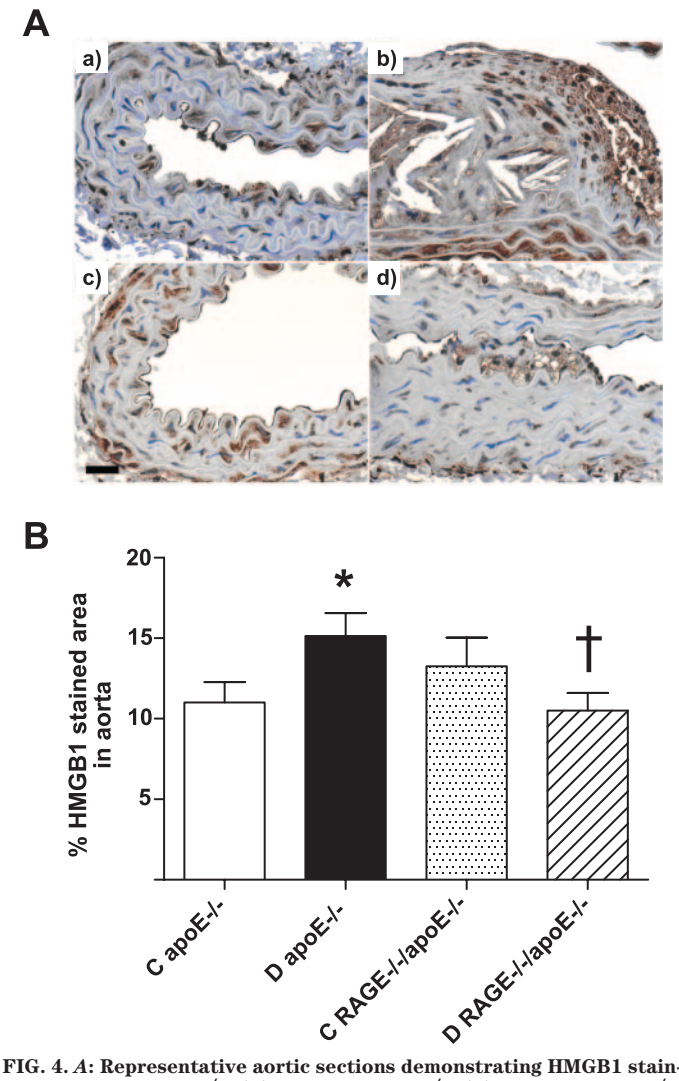

FIG. 4. *A*: Representative aortic sections demonstrating HMGB1 staining in control apoE$^{-/-}$ (*a*), diabetic apoE$^{-/-}$ (*b*), control RAGE$^{-/-}$/apoE$^{-/-}$ (*c*), and diabetic RAGE$^{-/-}$/apoE$^{-/-}$ (*d*) mice. Scale bar = 20 μm. *B*: Graph presenting percentage of HMGB1-positive aortic area in each group. *P < 0.05 vs. control apoE$^{-/-}$, †P < 0.05 vs. diabetic apoE$^{-/-}$. Data are expressed as means ± SE. (Please see http://dx.doi.org/10.2337/db07-1808 for a high-quality digital representation of this figure.)

femoral artery denudation (12). Furthermore, a recent study in apoE/RAGE double knockout mice has also demonstrated reduced plaque area, albeit in a nondiabetic context (23).

RAGE is pattern recognition receptor (1) that is able to bind a chemically diverse range of AGEs and other non-AGE ligands, including s100/calgranulins, HMGB1, and β-sheet fibrils. In atherosclerotic vascular disease, the expression of RAGE is focally increased (14,15,21), paralleling an accumulation in RAGE ligands. The major RAGE ligand in the context of diabetes remains to be established. However, the efficacy of AGE-reducing interventions, including alagebrium and aminoguanidine, on diabetes-associated atherosclerosis suggests that AGEs play a pivotal role (14). In this study, we demonstrate increased vascular accumulation of CML along with other RAGE ligands in diabetic apoE$^{-/-}$ mice. This increase in vascular CML was markedly attenuated in diabetic RAGE$^{-/-}$/apoE$^{-/-}$ mice, although the hyperglycemia and hyperlipidemia were not corrected. This decrease in vascular AGEs was not due to overexpression of AGE clearance receptors in RAGE$^{-/-}$/apoE$^{-/-}$ mice. In fact, diabetes-associated increases in *AGE-R1* (*OST-3*) and *AGE-R3* (*galactin-3*) were significantly attenuated in diabetic RAGE$^{-/-}$/apoE$^{-/-}$ mice, possibly reflecting reduced AGE accumulation in these animals. Expression of the type B macrophage scavenger receptor *CD36* (24) was also attenuated in diabetic RAGE$^{-/-}$/apoE$^{-/-}$ mice. Although this change is likely to be secondary to reduced leukocyte recruitment, CD36 has been clearly demonstrated to play a proatherogenic role because the absence of macrophage CD36 protects against vascular lesion formation in mice (25). Thus, one cannot exclude that some of the antiatherosclerotic effects seen with RAGE deletion could be related to changes in the expression of CD36.

Plaque accumulation in the diabetic apoE$^{-/-}$ mouse is closely correlated with the generation of ROS, which drive a number of proatherogenic processes, such as monocyte infiltration, smooth muscle cell recruitment, cell adhesion, and increased accumulation of AGEs, which are all observed in the diabetic apoE$^{-/-}$ plaque. For example, we

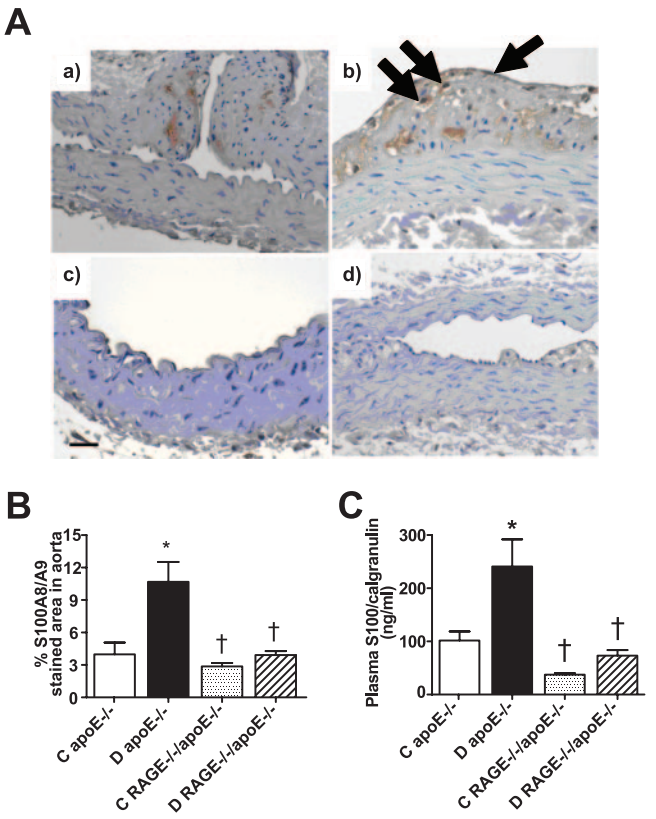

FIG. 5. ***A*****: Representative histological sections demonstrating increased S100A8/A9 staining, particularly in foam cells, endothelial cells (see arrow) and macrophages (see double arrow) in the diabetic apoE$^{-/-}$ aorta. Panel presents photomicrographs from aortic wall and plaques in control apoE$^{-/-}$ (*a*), diabetic apoE$^{-/-}$ (*b*), control RAGE$^{-/-}$/apoE$^{-/-}$ (*c*), and diabetic RAGE$^{-/-}$/apoE$^{-/-}$ (*d*) mice. Scale bar = 20 μm. *B*: Graph presenting percentage of S100A8/A9-positive aortic area in each group. *P < 0.05 vs. control apoE$^{-/-}$, †P < 0.01 vs. diabetic apoE$^{-/-}$. *C*: Plasma levels of S100A8/A9 are increased in diabetic apoE$^{-/-}$ mice compared with control apoE$^{-/-}$ and RAGE$^{-/-}$/apoE$^{-/-}$. *P < 0.01 vs. control apoE$^{-/-}$, †P < 0.001 vs. diabetic apoE$^{-/-}$. Data are means ± SE. (Please see http://dx.doi.org/10.2337/db07-1808 for a high-quality digital representation of this figure.)**

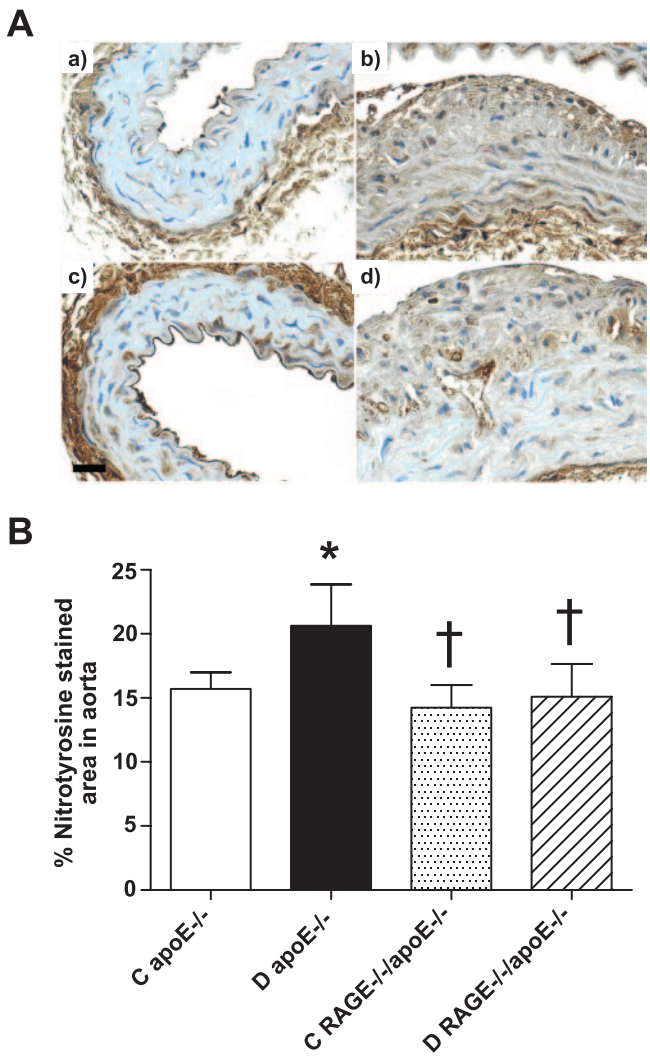

FIG. 6. ***A*****: Nitrotyrosine expression is enhanced in diabetic apoE$^{-/-}$ aorta indicative of increased oxidative stress. Representative aortic sections showing nitrotyrosine staining in control apoE$^{-/-}$ (*a*), diabetic apoE$^{-/-}$ (*b*), control RAGE$^{-/-}$/apoE$^{-/-}$ (*c*), and diabetic RAGE$^{-/-}$/apoE$^{-/-}$ (*d*) mice. Scale bar = 20 μm. *B*: Graph presenting percentage of nitrotyrosine-positive aortic area in each group. *P < 0.05 vs. control apoE$^{-/-}$, †P < 0.05 vs. diabetic apoE$^{-/-}$. Data are means ± SE. (Please see http://dx.doi.org/10.2337/db07-1808 for a high-quality digital representation of this figure.)**

have recently shown that increased oxidative stress in GPx1$^{-/-}$/apoE$^{-/-}$ mice accelerates diabetes-associated atherosclerosis via upregulation of proinflammatory and profibrotic pathways (26). The role of RAGE as a mediator of oxidative stress in diabetes was also observed in the present study. In our study, diabetes was associated with increases in vascular oxidative stress, as demonstrated by aortic nitrotyrosine staining. This probably occurred partly as a result of increased expression of *p47phox* and *gp91phox*, subunits of NAPDH oxidase, and *rac1*, a GTPase involved in NADPH oxidase activation. Expression of the NADPH subunits as well as nitrotyrosine staining were significantly attenuated in diabetic RAGE$^{-/-}$/apoE$^{-/-}$ mice. Furthermore, aortic gene expression of the AT1a receptor, which is known to enhance ROS generation via NADPH oxidase (27), was increased in diabetic apoE$^{-/-}$ mice yet was significantly reduced in the diabetic RAGE$^{-/-}$/apoE$^{-/-}$ mice.

RAGE activation is involved not only in the acceleration of atherosclerotic lesion formation but also in promoting proinflammatory pathways considered to play an important role in diabetes-accelerated atherosclerosis. For example, the diabetic plaque is characterized by the increased expression of inflammatory cytokines, chemokines and adhesion molecules that promote leukocyte infiltration and foam cell accumulation. This inflammatory response was clearly attenuated in the diabetic RAGE$^{-/-}$/apoE$^{-/-}$ mice, as reflected by decreased accumulation of macrophages and T-cells and reduced aortic expression of related chemokines, cytokines, and adhesion molecules. A number of different components contribute to RAGE-induced inflammation, including oxidative stress and AGE accumulation. However, one key mediator appears to be activation of the proinflammatory transcription factor NF-κB, because RAGE has the unique ability to sustain NF-κB activation through de novo synthesis of NF-κB p65-mRNA and to provide a constantly growing pool of transcriptional active NF-κB (28). The downstream effects of this pathway include activation of NADPH oxidase, VCAM-1, and tissue factor and the autoinduction of RAGE expression in a positive feedback loop (29). In our study, the expression of the NF-κB subunit p65 was upregulated in the diabetic apoE$^{-/-}$ aorta. By contrast, diabetes-associated upregulation of NF-κB and subsequent NF-κB–dependent expression of proinflammatory genes were

attenuated in diabetic RAGE$^{-/-}$/apoE$^{-/-}$ mice. To complement the finding with respect to NF-κB, we measured gene expression of the NF-κB–dependent protein, *MCP-1*. *MCP-1* gene expression was increased at least sixfold in the diabetic apoE$^{-/-}$ mice, and this increase was significantly attenuated in the RAGE$^{-/-}$/apoE$^{-/-}$ mice in association with reduced macrophage infiltration.

In the present study, increased gene expression of various collagens was observed in diabetic apoE$^{-/-}$ mice. This result complements previous findings by several groups, including our own by demonstrating increased matrix accumulation as assessed by picrosirius red or increased collagen protein expression as assessed immunohistochemically (9,14). RAGE deletion in these diabetic apoE$^{-/-}$ mice particularly influenced collagen III gene expression, a finding similar to that seen previously with two chemically disparate AGE inhibitors (14). With respect to *MMP-9* expression, the increase in mRNA levels in these diabetic apoE$^{-/-}$ mice complements findings by another group that specifically examined *MMP-9* expression and activity (9). Furthermore, the decrease in *MMP-9* expression seen in the diabetic RAGE$^{-/-}$/apoE$^{-/-}$ mice is similar to that seen previously in studies using sRAGE (9). Previously, it has been suggested that the changes observed with respect to matrix and MMP expression in response to inhibition of RAGE may reflect stabilization of the plaque. Nevertheless, the long-term implications of the changes in MMPs and collagens seen in this model remain controversial because this is not considered a model of plaque rupture.

The clear vasculoprotection observed in the diabetic RAGE$^{-/-}$/apoE$^{-/-}$ mice further support previous experimental studies showing that blockade of RAGE activation, either with neutralizing antibodies or sRAGE (8,9,12), prevents the initiation and progression of atheroma formation in diabetic mice. It is noteworthy that in our study, both full-length and truncated isoforms of RAGE were absent in RAGE$^{-/-}$/apoE$^{-/-}$ mice. Because RAGE has been reported to not only bind to AGEs but also to other ligands such as HMGB1 and certain S100 isoforms, these ligands were examined in this study. S100 A8/9 levels were increased in the plasma and aortic tissues in diabetic apoE$^{-/-}$ mice, and this increase was not observed in the RAGE$^{-/-}$/apoE$^{-/-}$ double knockout mice, even in the presence of concomitant diabetes. A similar upregulation of HMGB1 in the aorta of diabetic mice was also not seen in vessels from RAGE$^{-/-}$/apoE$^{-/-}$ mice. However, the circulating levels of HMGB1 were higher in the double knockout mice. This finding is unexplained but may occur because RAGE$^{-/-}$/apoE$^{-/-}$ mice have no sRAGE to bind HMBG from the circulation, thus enhancing accumulation of this protein within the plasma. These findings extend recent in vitro studies, albeit in a nondiabetic context, describing effects of various RAGE ligands on chemokines, adhesion molecules, and MMPs, including MCP-1, VCAM-1, and MMP-2 (23).

The finding that atherosclerosis was attenuated even in the absence of potentially protective circulating sRAGE strongly supports the postulate that the major mechanism of action of sRAGE is local antagonism of RAGE-dependent signaling. The importance of the full-length RAGE receptor in inflammatory vascular injury, even in the nondiabetic context, is suggested by the finding that even in control RAGE$^{-/-}$/apoE$^{-/-}$ mice, there was reduced plaque accumulation, as was recently reported by another group (23).

In summary, this study demonstrates that accelerated atherosclerotic plaque accumulation associated with diabetes is prevented in the absence of RAGE. The antiatherosclerotic effects seen in diabetic RAGE$^{-/-}$/apoE$^{-/-}$ mice were associated with reduced expression of a range of proatherogenic factors, including ROS and inflammatory cytokines, ultimately leading to reduced leukocyte recruitment. Thus, these data provide further support for the development of novel therapies that target RAGE activation in the prevention and treatment of diabetic macrovascular complications.

ACKNOWLEDGMENTS

A.S.-P. has received grants from the Academy of Finland, the Orion-Farmos Research Foundation, and the Finnish Cardiovascular Research Foundation. A.K. has received support from Association de Langue Française pour l'Etude du Diabète et des Maladies Métaboliques (France). M.T. has received grants from the Juvenile Diabetes Research Foundation (JDRF) Center, NHMRC, National Health Fund (NHF), and the National Institutes of Health (5R0-HL-083452-02); a Career Development Award (NHMRC/Diabetes Australia); and the Kidney Health Australia-Bootle bequest. J.M.F. has received grants from the JDRF Center, NHMRC, NHF, and the National Institutes of Health (5R0-HL-083452-02) and is a recipient of a JDRF career development award. P.P.N. has received grants from the JDRF Center and the Deutsche Forschungs-gemeinschaft (SFB405). A.B. has received a JDRF Center grant. M.E.C. has received grants from the JDRF Center, NHMRC, NHF, and the National Institutes of Health (5R0-HL-083452-02). K.A.J.-D. has received grants from the JDRF Center, NHMRC, NHF, and the National Institutes of Health (5R0-HL-083452-02) and is a recipient of a NHMRC/NHF career development award.

We thank Maryann Arnstein for excellent technical assistance and Kylie Gilbert and Steve Risis for their expertise in caring for the animals for the duration of the study.

REFERENCES

1. Bierhaus A, Humpert PM, Morcos M, Wendt T, Chavakis T, Arnold B, Stern DM, Nawroth PP: Understanding RAGE, the receptor for advanced glycation end products. *J Mol Med* 83:876–886, 2005
2. Yonekura H, Yamamoto Y, Sakurai S, Petrova RG, Abedin MJ, Li H, Yasui K, Takeuchi M, Makita Z, Takasawa S, Okamoto H, Watanabe T, Yamamoto H: Novel splice variants of the receptor for advanced glycation end-products expressed in human vascular endothelial cells and pericytes, and their putative roles in diabetes-induced vascular injury. *Biochem J* 370: 1097–1109, 2003
3. Wendt TM, Tanji N, Guo J, Kislinger TR, Qu W, Lu Y, Bucciarelli LG, Rong LL, Moser B, Markowitz GS, Stein G, Bierhaus A, Liliensiek B, Arnold B, Nawroth PP, Stern DM, D'Agati VD, Schmidt AM: RAGE drives the development of glomerulosclerosis and implicates podocyte activation in the pathogenesis of diabetic nephropathy. *Am J Pathol* 162:1123–1137, 2003
4. Shoji T, Koyama H, Morioka T, Tanaka S, Kizu A, Motoyama K, Mori K, Fukumoto S, Shioi A, Shimogaito N, Takeuchi M, Yamamoto Y, Yonekura H, Yamamoto H, Nishizawa Y: Receptor for advanced glycation end products is involved in impaired angiogenic response in diabetes. *Diabetes* 55:2245–2255, 2006
5. Bierhaus A, Haslbeck KM, Humpert PM, Liliensiek B, Dehmer T, Morcos M, Sayed AA, Andrassy M, Schiekofer S, Schneider JG, Schulz JB, Heuss D, Neundorfer B, Dierl S, Huber J, Tritschler H, Schmidt AM, Schwaninger M, Haering HU, Schleicher E, Kasper M, Stern DM, Arnold B, Nawroth PP: Loss of pain perception in diabetes is dependent on a receptor of the immunoglobulin superfamily. *J Clin Invest* 114:1741–1751, 2004
6. Myint KM, Yamamoto Y, Doi T, Kato I, Harashima A, Yonekura H,

Watanabe T, Shinohara H, Takeuchi M, Tsuneyama K, Hashimoto N, Asano M, Takasawa S, Okamoto H, Yamamoto H: RAGE control of diabetic nephropathy in a mouse model: effects of RAGE gene disruption and administration of low-molecular weight heparin. *Diabetes* 55:2510–2522, 2006
7. Yamamoto Y, Kato I, Doi T, Yonekura H, Ohashi S, Takeuchi M, Watanabe T, Yamagishi S, Sakurai S, Takasawa S, Okamoto H, Yamamoto H: Development and prevention of advanced diabetic nephropathy in RAGE-overexpressing mice. *J Clin Invest* 108:261–268, 2001
8. Park L, Raman KG, Lee KJ, Lu Y, Ferran LJ Jr, Chow WS, Stern D, Schmidt AM: Suppression of accelerated diabetic atherosclerosis by the soluble receptor for advanced glycation endproducts. *Nat Med* 4:1025–1031, 1998
9. Bucciarelli LG, Wendt T, Qu W, Lu Y, Lalla E, Rong LL, Goova MT, Moser B, Kislinger T, Lee DC, Kashyap Y, Stern DM, Schmidt AM: RAGE blockade stabilizes established atherosclerosis in diabetic apolipoprotein E-null mice. *Circulation* 106:2827–2835, 2002
10. Wautier JL, Schmidt AM: Protein glycation: a firm link to endothelial cell dysfunction. *Circ Res* 95:233–238, 2004
11. Fu MX, Wells-Knecht KJ, Blackledge JA, Lyons TJ, Thorpe SR, Baynes JW: Glycation, glycoxidation, and cross-linking of collagen by glucose: kinetics, mechanisms, and inhibition of late stages of the Maillard reaction. *Diabetes* 43:676–683, 1994
12. Sakaguchi T, Yan SF, Yan SD, Belov D, Rong LL, Sousa M, Andrassy M, Marso SP, Duda S, Arnold B, Liliensiek B, Nawroth PP, Stern DM, Schmidt AM, Naka Y: Central role of RAGE-dependent neointimal expansion in arterial restenosis. *J Clin Invest* 111:959–972, 2003
13. Candido R, Jandeleit-Dahm KA, Cao Z, Nesteroff SP, Burns WC, Twigg SM, Dilley RJ, Cooper ME, Allen TJ: Prevention of accelerated atherosclerosis by angiotensin-converting enzyme inhibition in diabetic apolipoprotein E-deficient mice. *Circulation* 106:246–253, 2002
14. Forbes JM, Yee LT, Thallas V, Lassila M, Candido R, Jandeleit-Dahm KA, Thomas MC, Burns WC, Deemer EK, Thorpe SM, Cooper ME, Allen TJ: Advanced glycation end product interventions reduce diabetes-accelerated atherosclerosis. *Diabetes* 53:1813–1823, 2004
15. Calkin AC, Forbes JM, Smith CM, Lassila M, Cooper ME, Jandeleit-Dahm KA, Allen TJ: Rosiglitazone attenuates atherosclerosis in a model of insulin insufficiency independent of its metabolic effects. *Arterioscler Thromb Vasc Biol* 25:1903–1909, 2005
16. Liliensiek B, Weigand MA, Bierhaus A, Nicklas W, Kasper M, Hofer S, Plachky J, Grone HJ, Kurschus FC, Schmidt AM, Yan SD, Martin E, Schleicher E, Stern DM, Hammerling GG, Nawroth PP, Arnold B: Receptor for advanced glycation end products (RAGE) regulates sepsis but not the adaptive immune response. *J Clin Invest* 113:1641–1650, 2004
17. Cefalu WT, Wang ZQ, Bell-Farrow A, Kiger FD, Izlar C: Glycohemoglobin measured by automated affinity HPLC correlates with both short-term and long-term antecedent glycemia. *Clin Chem* 40:1317–1321, 1994
18. Candido R, Allen TJ, Lassila M, Cao Z, Thallas V, Cooper ME, Jandeleit-Dahm KA: Irbesartan but not amlodipine suppresses diabetes-associated atherosclerosis. *Circulation* 109:1536–1542, 2004
19. Goldin A, Beckman JA, Schmidt AM, Creager MA: Advanced glycation end products: sparking the development of diabetic vascular injury. *Circulation* 114:597–605, 2006
20. Kovanen P: Mast cells: multipotent local effector cells in atherothrombosis. *Immunol Rev* 217:105–122, 2007
21. Andrassy M, Igwe J, Autschbach F, Volz C, Remppis A, Neurath MF, Schleicher E, Humpert PM, Wendt T, Liliensiek B, Morcos M, Schiekofer S, Thiele K, Chen J, Kientsch-Engel R, Schmidt AM, Stremmel W, Stern DM, Katus HA, Nawroth PP, Bierhaus A: Posttranslationally modified proteins as mediators of sustained intestinal inflammation. *Am J Pathol* 169:1223–1237, 2006
22. Thomas MC, Tikellis C, Burns WM, Bialkowski K, Cao Z, Coughlan MT, Jandeleit-Dahm K, Cooper ME, Forbes JM: Interactions between renin angiotensin system and advanced glycation in the kidney. *J Am Soc Nephrol* 17:2976–2984, 2005
23. Harja E, Bu DX, Hudson BI, Chang JS, Shen X, Hallam K, Kalea AZ, Lu Y, Rosario RH, Oruganti S, Nikolla Z, Belov D, Lalla E, Ramasamy R, Yan SF, Schmidt AM: Vascular and inflammatory stresses mediate atherosclerosis via RAGE and its ligands in apoE−/− mice. *J Clin Invest* 118:183–194, 2008
24. Febbraio M, Silverstein RL: CD36: Implications in cardiovascular disease. *Int J Biochem Cell Biol* 23:23, 2007
25. Febbraio M, Guy E, Silverstein RL: Stem cell transplantation reveals that absence of macrophage CD36 is protective against atherosclerosis. *Arterioscler Thromb Vasc Biol* 24:2333–2338, 2004
26. Lewis P, Stefanovic N, Pete J, Calkin AC, Giunti S, Thallas-Bonke V, Jandeleit-Dahm KA, Allen TJ, Kola I, Cooper ME, de Haan JB: Lack of the antioxidant enzyme glutathione peroxidase-1 accelerates atherosclerosis in diabetic apolipoprotein E-deficient mice. *Circulation* 115:2178–2187, 2007
27. Griendling KK, Minieri CA, Ollerenshaw JD, Alexander RW: Angiotensin II stimulates NADH and NADPH oxidase activity in cultured vascular smooth muscle cells. *Circ Res* 74:1141–1148, 1994
28. Bierhaus A, Schiekofer S, Schwaninger M, Andrassy M, Humpert PM, Chen J, Hong M, Luther T, Henle T, Kloting I, Morcos M, Hofmann M, Tritschler H, Weigle B, Kasper M, Smith M, Perry G, Schmidt AM, Stern DM, Haring HU, Schleicher E, Nawroth PP: Diabetes-associated sustained activation of the transcription factor nuclear factor-κB. *Diabetes* 50:2792–2808, 2001
29. Li J, Schmidt AM: Characterization and functional analysis of the promoter of RAGE, the receptor for advanced glycation end products. *J Biol Chem* 272:16498–16506, 1997